PHYSICAL REVIEW B **84**, 085311 (2011)

Spin-polarized half-metallic state of a ferromagnetic δ layer in a semiconductor host

S. Caprara,[1,2] V. V. Tugushev,[3,4] and E. V. Chulkov[1,4]

[1]*Donostia International Physics Center (DIPC), P. de Manuel Lardizabal 4, 20018 San Sebastián, Basque Country, Spain*
[2]*Dipartimento di Fisica, Università di Roma "La Sapienza," Piazzale Aldo Moro 2, 00185 Rome, Italy*
[3]*RRC Kurchatov Institute, Kurchatov Square 1, 123182 Moscow, Russia*
[4]*Departamento de Física de Materiales, Facultad de Ciencias Químicas, UPV/EHU and Centro Mixto CSIC-UPV/EHU, Apartado 1072, 20080 San Sebastián, Basque Country, Spain*

(Received 11 April 2011; revised manuscript received 30 May 2011; published 23 August 2011)

We discuss a model which is apt to describe the appearance of a spin-polarized half-metallic state around a single δ layer of a magnetic transition metal embedded into a nonmagnetic semiconductor host. We show that ferromagnetism in this system can be attributed to the intrinsic physical properties of the δ layer. The relevant physical effects described by our model are the hybridization of the electron states of the metal and semiconductor atoms, the charge redistribution around the δ layer, and the electron-electron correlation on a metal atom, which is the driving force of ferromagnetism. We obtain the mean-field phase diagram of the model at zero and finite temperature, both in the case when the chemical potential is fixed, and when the density of particles on the δ layer is fixed. The relevance of our results in connection with numerical and experimental results on the so-called digital magnetic heterostructures, in the absence and in the presence of a quantum-well carrier channel, is eventually discussed.

DOI: 10.1103/PhysRevB.84.085311 PACS number(s): 73.40.Sx, 75.70.Cn, 75.10.Lp

I. INTRODUCTION

Hybrid heterostructures containing (sub)monolayers of a magnetic transition metal (the so-called magnetic δ layers) embedded into a normal semiconductor host are nowadays the object of increasing interest both on purely theoretical grounds and in view of possible applications in spintronics. Such systems [called *digital magnetic heterostrucutres* (DMHs)] contain either an isolated magnetic δ layer, or a regular array of δ layers. Combining magnetic and nonmagnetic layers with different carrier lifetimes and mobility in DMHs opens a new branch of hybrid metal/semiconductor nanostructure engineering.

The available experimental studies mostly refer to systems in which δ layers of Mn are inserted into a III-V semiconductor (GaAs or GaSb) host. These studies show that short- or long-range ferromagnetic (FM) order exists both in the case of an isolated δ layer[1] and in the case of a periodical array of such layers.[2,3] Little attention has been devoted, so far, to DMHs in which 3*d*-magnetic metal δ layers are inserted into a IV-group semiconductor (Si or Ge) host, although these systems are the more natural candidates to realize full integration of spintronics with standard Si-based electronics. While initially the magnetic properties of DMHs were attributed to the interplay of the different δ layers, or to the presence of free carriers in systems with a quantum-well carrier channel parallel to the δ layer,[4–6] increasing experimental evidence indicates that magnetism can be ascribed even to an individual δ layer,[2,7] while the channel or the periodic arrangement of δ layers may introduce some interesting modifications.

Ab initio calculations, instead, have been performed on DMHs with an array of Mn δ layers which is periodically arranged along the (001) direction of both a III-V semiconductor (Mn/GaAs, Ref. 8) and a IV-group semiconductor (Mn/Ge, Refs. 9 and 10; Mn/Si, Refs. 9,11, and 12; $Mn/Si_{0.5}Ge_{0.5}$, Ref. 9). In *all* these numerical studies three important results were obtained: (i) ferromagnetism is always more favorable than antiferromagnetism in the Mn δ layers; (ii) charge carriers are doped into the system and are confined in the vicinity of the Mn δ layers; (iii) the system displays a half-metallic electron spectrum with strongly spin-polarized nearly two-dimensional energy bands.

The question then arises whether these outcomes stem from a common physical origin and are related, e.g., to the peculiar geometry and to the content of the DMH. Indeed, the half-metallic state is usually an exception rather than the rule in bulk FM metals (as, e.g., in some Heisler alloys), where the simultaneous presence of narrow *d* bands and wide (s,p) bands makes the conditions for the full exchange splitting very unlikely to be met.

To provide an interpretation to the experimental results and to the outcomes of *ab initio* calculations and in the attempt to clarify the intimate connection which relates ferromagnetism, the occurrence of two-dimensional bands, and the half-metallic state, we introduce below an Anderson-like model for an isolated magnetic δ layer embedded into a semiconductor host. Rather than providing an accurate description of the band structure of such a system, we want to capture the relevant physical effects, as suggested by the numerical calculations, i.e., the hybridization between the (s,p) orbitals of the semiconductor and the *d* orbitals of the transition metal, the redistribution and confinement of charge carriers around the δ layer, and the strong electron-electron correlation on *d* orbitals, which promotes ferromagnetism. Despite the simplifying nature of our working assumptions, we are able to obtain transparent analytical results, which reproduce the main outcomes of numerical calculations. Moreover, since the parameters of the model can be varied independently, we are able to obtain a phase diagram of our model. We show that a half-metallic state may indeed occur near a magnetic δ layer, due to the formation of two-dimensional (confinement) electron bands below the band edge of the bulk semiconductor. For these bands, which are the cooperative result of (s,p)-*d*

hybridization and charge redistribution around the δ layer, the full exchange splitting in the FM state is possible and occurs for physically reasonable values of the exchange interaction. Our results also show that, in a wide region of parameter space, the spin-polarized half-metallic state might have a *ferrimagnetic* structure, with the spins of the spatially separated electron states of the metal and of the semiconductor aligned in opposite directions. The ground-state properties of the model have been studied earlier,[13] in the case when the chemical potential is fixed (i.e, within the grand-canonical statistical ensemble). Here, we provide more detail on the ground-state properties, discussing also the case in which the number of particles in the δ layer is fixed (within the canonical statistical ensemble). Within this respect, we point out that intermediate situations are likely to occur in real systems: although an isolated δ layer cannot change the particle content of the bulk semiconductor host, some of the carriers introduced by the d metal atoms may penetrate into the bulk semiconductor, abandoning the δ layer. The problem of charge redistribution in the system is very complicated and should take into account the Debye screening length in the system, the deformation of the band structure of the semiconductor near the δ layer, and the self-consistently determined modulation of the electrochemical potential. In the following, we account for charge redistribution around an isolated δ layer in a phenomenological way, through a local correction to the chemical potential, and analyze the two extreme situations of a fixed chemical potential (with the bulk semiconductor acting as a particle reservoir) and of a fixed number of particles in the δ layer (where all the particles stay confined in the proximity of the δ layer). We then extend our analysis to finite temperature, addressing the issue of thermodynamical fluctuations. Finally, we take into account the effect of charge redistribution when a quantum-well carrier channel is present in the system, parallel to the δ layer, considering the case in which the number of particles in the system composed by the δ layer and the quantum-well carrier channel is fixed.

The scheme of the paper is the following. In Sec. II we introduce our model. In Sec. III we analyze the ground-state properties of the model, recalling the results obtained at fixed chemical potential (Sec. III A) and discussing the case in which the number of particles in the δ layer is fixed (Sec. III B). In Sec. IV we discuss the case of finite temperatures : fixed chemical potential (Sec. IV A) and fixed number of particles (Sec. IV B). The role of thermodynamical fluctuations is discussed in Sec. V. In Sec. VI we analyze the effect of charge redistribution in the presence of a quantum-well carrier channel. Concluding remarks, perspectives, and a summary to our work are found in Sec. VII.

II. SETUP OF THE PROBLEM

To describe the spin-polarized half-metallic state which occurs in the vicinity of an isolated magnetic δ layer embedded into a semiconductor host, we include in our model only the relevant degrees of freedom and interactions. For instance, we neglect orbital degrees of freedom, which are responsible for the higher value of the spin on the d orbitals of t_g and e_g symmetry of the transition-metal atom, according to Hund's rule, but are not essential to explain the occurrence of a spin-polarized state. Positions within our system are characterized by the vectors $\mathbf{R} = (\mathbf{r}, z)$, where $\mathbf{r}$ is a two-dimensional position vector parallel to the δ layer and z is the coordinate in the perpendicular direction. The δ layer is ideally identified as the plane $z = 0$. This is a simplified description of a real δ layer, which has a finite thickness, with a smeared profile, due to the diffusion of Mn atoms into the semiconductor host. We shall come back to the possible drawbacks of this assumption in Sec. VI, when discussing the properties of a system with a quantum-well carrier channel parallel to the δ layer. In the following, we mostly use the term δ layer to indicate the ideal plane, unless otherwise specified. For wave vectors we adopt the same decomposition adopted for position vectors and write $\mathbf{K} = (\mathbf{k}, \kappa)$, where $\mathbf{k}$ is a two-dimensional wave vector parallel to the δ layer and κ is a one-dimensional wave vector perpendicular to it.

As a further simplifying assumption, we consider a case in which the valence band of the semiconductor is deep, and can be neglected, whereas the conduction band, arising from a single s orbital, is well described within the effective mass approximation. The Hamiltonian of the semiconductor host is therefore

$$\mathcal{H}_s = \sum_{\mathbf{K},\sigma} E_{\mathbf{K}}\, s^{\dagger}_{\mathbf{K},\sigma} s_{\mathbf{K},\sigma},$$

where $s^{(\dagger)}_{\mathbf{K},\sigma}$ annihilates (creates) an electron in a state characterized by a three-dimensional wave vector $\mathbf{K}$ and a spin projection $\sigma = \uparrow, \downarrow$ onto the quantization axis, and the dispersion law of the conduction band is

$$E_{\mathbf{K}} = \frac{\hbar^2 \mathbf{K}^2}{2m^*} = \frac{\hbar^2}{2m^*}(\mathbf{k}^2 + \kappa^2) \equiv E_{\mathbf{k}} + E_{\kappa},$$

where m^* is the effective mass of charge carriers near the bottom of the conduction band. The Hamiltonian of an isolated magnetic δ layer is

$$\mathcal{H}_d = \sum_{\mathbf{k},\sigma} \epsilon_d\, d^{\dagger}_{\mathbf{k},\sigma} d_{\mathbf{k},\sigma} + I \sum_i n_{d,\uparrow}(\mathbf{r}_i)\, n_{d,\downarrow}(\mathbf{r}_i), \qquad (1)$$

where $d^{(\dagger)}_{\mathbf{k},\sigma}$ annihilates (creates) an electron with two-dimensional wave vector $\mathbf{k}$ and spin projection $\sigma = \uparrow, \downarrow$ onto the quantization axis. As explained above, we assume a single doubly degenerate orbital on the transition-metal site, although we maintain the denomination of d orbital. We also neglect the small overlap of d orbitals at different sites, taking a dispersionless d band ϵ_d. This assumption is quite realistic, since in real systems the mobility of d electrons is mainly due to the hybridization with the (s, p) electron states of the semiconductor. The electron-electron correlation is described as a Hubbard interaction term of strength I between two electrons in the same d orbital, which promotes magnetism. We assume that the electrons are essentially localized at the transition-metal sites $\mathbf{r}_i$, and $n_{d,\sigma}(\mathbf{r}_i) = d^{\dagger}_{i,\sigma} d_{i,\sigma}$ represents the number of d electrons with spin projection σ on a given site $\mathbf{r}_i$ of the two-dimensional lattice formed by the transition-metal atoms within the δ layer. Here, $d^{(\dagger)}_{i,\sigma}$ is the annihilation (creation) operator of an electron in the corresponding atomic state.

When the magnetic δ layer is inserted into the semiconductor host, various physical effects arise. As suggested by *ab initio* calculations, we propose two effects to be relevant for the occurrence of a spin-polarized half-metallic state, namely, the hybridization between the electron states of the transition-metal atoms in the δ layer and the electron states in the semiconductor (within our model, *s-d* hybridization) $V(z;\mathbf{r}-\mathbf{r}')$, and charge redistribution within the semiconductor host around the δ layer. This latter effect should be determined self-consistently, but in our simplified treatment we describe it as a local correction to the chemical potential of s electrons, $U(z)$. Both these effects do not violate the translational invariance in the direction parallel to the δ layer, but break the translational invariance along the z axis. We approximate these two effects by means of contact terms at $\mathbf{r}=\mathbf{r}'$ and $z=0$, corresponding to the Hamiltonian

$$\mathcal{H}_\delta = \mathcal{H}_{s\text{-}d} + \mathcal{H}_{\rm loc} = \frac{1}{\sqrt{N_\perp}}\sum_{\mathbf{K},\sigma}(V d^\dagger_{\mathbf{k},\sigma} s_{\mathbf{K},\sigma} + \text{H.c.}) + \frac{U}{N_\perp}\sum_{\substack{\mathbf{K},\mathbf{K}'\\ \sigma}} \delta_{\mathbf{k},\mathbf{k}'} s^\dagger_{\mathbf{K},\sigma} s_{\mathbf{K}',\sigma},$$

where $N_\perp$ is the number of wave vectors κ allowed by the boundary conditions within the first Brillouin zone. It is worth noting that the first term describes a set of independent one-dimensional Anderson models, labeled by the dummy index $\mathbf{k}$.

We adopt for the Hubbard term in Eq. (1) the Hartree-Fock linearization

$$n_{d,\uparrow}(\mathbf{r}_i)n_{d,\downarrow}(\mathbf{r}_i) \to n_{d,\uparrow}\, n_{d,\downarrow}(\mathbf{r}_i) + n_{d,\downarrow}\, n_{d,\uparrow}(\mathbf{r}_i) - n_{d,\uparrow}n_{d,\downarrow},$$

where $n_{d,\sigma} = \langle n_{d,\sigma}(\mathbf{r}_i)\rangle$ is the average number of electrons with spin projection σ in the d orbital of a transition-metal atom. This factorization results in two spin-dependent Hartree d levels $\epsilon_{d,\sigma} = \epsilon_d + I n_{d,-\sigma}$ on the transition-metal atom. Supported also by the outcomes of *ab initio* calculations, we consider in the following the case of a generic filling of the magnetic δ layer and discard the possibility for antiferromagnetic (AFM) or incommensurate order, which require particular nesting conditions in the δ-layer band structure and are seemingly unlikely for an isolated δ layer.

The quantum-mechanical problem associated with the full Hamiltonian $\mathcal{H} = \mathcal{H}_s + \mathcal{H}_d + \mathcal{H}_\delta$, after the Hartree-Fock linearization of the Hubbard term, is reduced to an effective (self-consistent) one-body problem. Standard diagrammatic techniques yield the Green's functions

$$G_{dd,\sigma}(\zeta,\mathbf{k}) = \frac{[1-D(\zeta,\mathbf{k})]G^0_{dd,\sigma}(\zeta)}{1 - D(\zeta,\mathbf{k}) - \dfrac{|V|^2}{U}D(\zeta,\mathbf{k})G^0_{dd,\sigma}(\zeta)}$$

and

$$G_{ss,\sigma}(\zeta,\mathbf{k};\kappa,\kappa') = G^0_{ss}(\zeta,\mathbf{k};\kappa)\delta_{\kappa,\kappa'} + \frac{1}{N_\perp}G^0_{ss}(\zeta,\mathbf{k};\kappa)G^0_{ss}(\zeta,\mathbf{k};\kappa') \times \frac{U + |V|^2 G^0_{dd,\sigma}(\zeta)}{1 - D(\zeta,\mathbf{k}) - \dfrac{|V|^2}{U}D(\zeta,\mathbf{k})G^0_{dd,\sigma}(\zeta)},$$

where ζ henceforth indicates the complex frequency. Here,

$$G^0_{dd,\sigma}(\zeta) \equiv \frac{1}{\zeta - \epsilon_{d,\sigma}}$$

is the Green's function of electrons in an isolated magnetic δ layer, so that the related self-energy is

$$\Sigma_d(\zeta,\mathbf{k}) \equiv \left[G^0_{dd,\sigma}(\zeta)\right]^{-1} - \left[G_{dd,\sigma}(\zeta,\mathbf{k})\right]^{-1} = \frac{|V|^2}{U}\frac{D(\zeta,\mathbf{k})}{1-D(\zeta,\mathbf{k})},$$

$$G^0_{ss}(\zeta,\mathbf{k};\kappa) \equiv \frac{1}{\zeta - (E_\mathbf{k} + E_\kappa)} \equiv \frac{1}{\zeta - E_\mathbf{K}}$$

is the Green's function of electrons in the semiconductor, in the absence of the magnetic δ layer,

$$D(\zeta,\mathbf{k}) \equiv \frac{U}{N_\perp}\sum_\kappa G^0_{ss}(\zeta,\mathbf{k};\kappa) = \frac{iu}{\sqrt{\zeta - E_\mathbf{k}}},$$

where $u \equiv -\frac{\pi}{2}U W_z^{-1/2}$, and $(m^* W_z)^{-1/2}$ is a characteristic cutoff for the wave vector κ. This result is obtained observing that $G^0_{ss}(\zeta,\mathbf{k};\kappa)$ depends on the perpendicular wave vector κ through the one-dimensional dispersion law E_κ, and the sum over κ can be transformed into an energy integral with respect to the variable $E_\perp = E_\kappa$, with density of states $\mathcal{N}_\perp(E_\perp) \propto \sqrt{E_\perp}$.

The equation $D(\zeta,\mathbf{k}) = 1$ describes two-dimensional bound states (for $U<0$, i.e., $u>0$) or antibound states (for $U>0$, i.e., $u<0$) formed near the edge of the conduction band of the semiconductor due to the charge redistribution around the δ layer. Such states are localized in the z direction and propagating in the direction parallel to the δ layer. In the following, we treat the case $u>0$, when bound states at energies $\varepsilon_\mathbf{k} = E_\mathbf{k} - u^2$ are split off the bottom of the conduction band of the semiconductor. The explicit expressions of the Green's functions G_{sd} and G_{ds} are not required in the forthcoming discussion and shall be omitted.

The *s-d* hybridization V removes the poles of the s Green's function in correspondence with the bound states $\varepsilon_\mathbf{k}$ and promotes instead the formation of two two-dimensional *s-d* bands, which appear as poles of $G_{dd,\sigma}(\zeta,\mathbf{k})$ and $G_{ss,\sigma}(\zeta,\mathbf{k};\kappa,\kappa')$. The corresponding electron states are propagating in the direction parallel to the δ layer and confined in the z direction. We point out that the upper two-dimensional band may partially overlap the three-dimensional continuum at positive energy.

The Green's functions depend on the two-dimensional wave vector $\mathbf{k}$ through the two-dimensional dispersion law $E_\mathbf{k}$ and on the perpendicular wave vector κ through the one-dimensional dispersion law E_κ. Sums over momenta of the Green's functions can be calculated explicitly after transformation into energy integrals with respect to the variables $E_\parallel = E_\mathbf{k}$ and $E_\perp = E_\kappa$, with density of states $\mathcal{N}_\parallel(E_\parallel) =$ constant and $\mathcal{N}_\perp(E_\perp) \propto \sqrt{E_\perp}$, respectively. The results of these calcula-

tions are listed hereafter:

$$\bar{G}_{dd,\sigma}(\zeta) \equiv \frac{1}{N_\parallel}\sum_{\mathbf{k}} G_{dd,\sigma}(\zeta,\mathbf{k}) = \frac{\Phi_\sigma(\zeta;\zeta)-\Phi_\sigma(\zeta-W;\zeta)}{W},$$

where $N_\parallel$ is the number of $\mathbf{k}$ vectors allowed within the first Brillouin zone by the boundary conditions, W is the width of the two-dimensional band dispersion $E_\mathbf{k}$, the function

$$\Phi_\sigma(Z;\zeta) \equiv Z G^0_{dd,\sigma}(\zeta) - 2v\left[G^0_{dd,\sigma}(\zeta)\right]^2\left\{i\sqrt{Z} - \left[u - vG^0_{dd,\sigma}(\zeta)\right]\ln\left[u + i\sqrt{Z} - vG^0_{dd,\sigma}(\zeta)\right]\right\}$$

depends on two complex frequency arguments, Z and ζ, and $v \equiv -|V|^2 u/U = \frac{\pi}{2}|V|^2 W_z^{-1/2} > 0$ [hence, the d self-energy reads $\Sigma_d(\zeta,\mathbf{k}) = v/(u + i\sqrt{\zeta - E_\mathbf{k}})$];

$$\bar{G}_{ss,\sigma}(\zeta) \equiv \frac{1}{N_\parallel}\sum_{\mathbf{k},\kappa} G_{ss,\sigma}(\zeta,\mathbf{k};\kappa,\kappa) = \frac{\Psi_\sigma(\zeta;\zeta)-\Psi_\sigma(\zeta-W;\zeta)}{W},$$

with the function

$$\Psi_\sigma(Z;\zeta) \equiv \ln\frac{u + i\sqrt{Z} - vG^0_{dd,\sigma}(\zeta)}{i\sqrt{Z}} - i\pi N_\perp\sqrt{\frac{Z}{W_z}},$$

depending on two complex frequency arguments, Z and ζ, and the last term describing the three-dimensional conduction band of the semiconductor host. The density of states needed for the forthcoming calculations are then found as

$$\mathcal{N}_{\alpha,\sigma}(\omega) \equiv -\frac{1}{\pi}\mathrm{Im}\,\bar{G}_{\alpha\alpha,\sigma}(\zeta = \omega + i\delta),$$

with $\alpha = s,d$ and $\delta = 0^+$. In our numerical analysis we adopt the value $\delta = 10^{-3}W$, which is two orders of magnitude smaller than all other energy scales that characterize the system. The total density of states with spin projection $\sigma = \uparrow,\downarrow$ is

$$\mathcal{N}_\sigma(\omega) = \mathcal{N}_{d,\sigma}(\omega) + \mathcal{N}_{s,\sigma}(\omega). \quad (2)$$

A remark is in order, before proceeding to discuss the properties of our model. In typical experimental conditions the transition-metal (e.g., Mn) coverage is far from full. The transition-metal atoms therefore form a two-dimensional effective crystal with an average lattice spacing a^* which is larger than the typical lattice spacing a of the semiconductor host. In these conditions, the two-dimensional projection of the Brillouin zone of the host is folded a^*/a times and the spectrum is reorganized in subbands. Since integrals in $\mathbf{k}$ space are normalized to the area of the two-dimensional Brillouin zone associated with the lattice of transition-metal atoms, W is to be taken as the bandwidth of the lowest subband, which is as an order of magnitude reduced by a factor $(a/a^*)^2$ with respect to the width of the conduction band of the semiconductor host parallel to the δ layer.

III. GROUND-STATE PROPERTIES

A. Fixed chemical potential

We start our analysis by recalling the properties of the system at fixed chemical potential μ and zero temperature (i.e., when the system is described within the grand-canonical statistical ensemble and the chemical potential acts as a tunable control parameter) that have been briefly discussed earlier.[13] We provide here a more detailed description and a closer insight. Having fixed the reference energy level at the bottom the three-dimensional conduction band of the semiconductor host, $E_\mathbf{K} \geqslant 0$, we limit ourselves to discuss the case $\mu \leqslant 0$, since there are no free carriers in the system.

When the system is spin polarized, the population of particles with spin projection $\uparrow$ is different from the population of particles with spin projection $\downarrow$. The source of this unbalance is self-consistently related to the exchange splitting of the d level, $\Delta \equiv \epsilon_{d,\uparrow} - \epsilon_{d,\downarrow}$, where $\epsilon_{d,\sigma} = \epsilon_d + I n_{d,-\sigma}$. Indeed, the density of states for particles with spin projection σ, $\mathcal{N}_{\alpha,\sigma}(\omega)$, depends self-consistently on the number of particles with opposite spin projection on a transition-metal site, $n_{d,-\sigma}$. The two coupled self-consistency equations which determine $n_{d,\sigma}$ have the form

$$n_{d,\sigma} = \int_{-\infty}^{\mu} d\omega\,\mathcal{N}_{d,\sigma}(\omega) \equiv \Upsilon(n_{d,-\sigma}),$$

with $\sigma = \uparrow,\downarrow$. By expressing, e.g., $n_{d,\downarrow}$ as a function of $n_{d,\uparrow}$ and then substituting the formal expression into the equation for $n_{d,\uparrow}$, the two equations are decoupled, and a single equation of the form $n_{d,\uparrow} = \Lambda(n_{d,\uparrow}) \equiv \Upsilon(\Upsilon(n_{d,\uparrow}))$ is obtained. Although the expression of the function $\Lambda(n_{d,\uparrow})$ is rather involved, the equation for the single variable $n_{d,\uparrow}$ can be solved very efficiently by iterative bisection. Once the self-consistent value of $n_{d,\uparrow}$ is found, one can immediately proceed to evaluate $n_{d,\downarrow}$ and then the number of s electrons per transition-metal site with spin projection $\sigma = \uparrow,\downarrow$,

$$n_{s,\sigma} = \int_{-\infty}^{\mu} d\omega\,\mathcal{N}_{s,\sigma}(\omega).$$

The thermodynamic grand-canonical potential per transition-metal site can be calculated as

$$\Omega = \sum_{\substack{\alpha = s,d\\ \sigma = \uparrow,\downarrow}}\int_{-\infty}^{\mu} d\omega(\omega - \mu)\mathcal{N}_{\alpha,\sigma}(\omega) - I\,n_{d,\downarrow}\,n_{d,\uparrow},$$

where the last term prevents double counting of the Hartree energy. The (meta)stable phases correspond to (local) minima of Ω. In the case of coexistence of various minima for a given set of parameters, the most stable phase corresponds to the lowest value of Ω, while the other phases are metastable.

We do not aim here at an accurate fit of the band structure of a particular system, and rather want to discuss the general conditions which lead to the formation of a half-metallic spin-polarized state. Therefore, we adopted the set of parameters $\epsilon_d/W = -0.5$, $u/W^{1/2} = 1.0$, and $v/W^{3/2} = 0.05$, which allows one to capture the overall qualitative behavior of the numerical results (see, e.g., Ref. 8). We discuss now the properties of our model with varying μ and I. Typical behaviors of the self-consistent density of states, Eq. (2), that

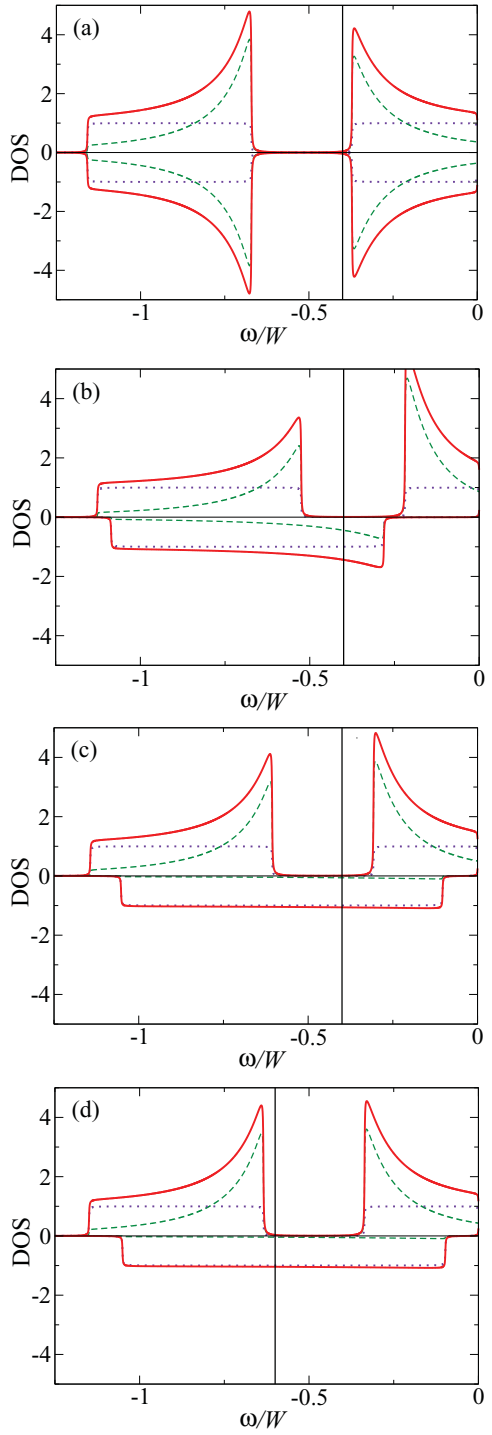

FIG. 1. (Color online) Density of states (DOS) per transition-metal site in units of W^{-1} vs ω/W for majority spins (plotted with positive sign) and minority spins (plotted with negative sign). The parameters are $\epsilon_d/W = -0.5$, $u/W^{1/2} = 1.0$, and $v/W^{3/2} = 0.05$, and (a) $I/W = 0.0$, $\mu/W = -0.4$ (PM state, see text); (b) $I/W = 1.5$, $\mu/W = -0.4$ (fm state, see text); (c) $I/W = 3.0$, $\mu/W = -0.4$ (fm state, see text); (d) $I/W = 3.0$, $\mu/W = -0.6$ (FM state, see text). Within each panel, the vertical line marks the position of the chemical potential. Solid (online red) lines mark the full DOS [$\mathcal{N}_\sigma(\omega)$, Eq. (2)], dashed (online green) lines mark the d contribution [$\mathcal{N}_{d,\sigma}(\omega)$], and dotted (online violet) lines mark the s contribution [$\mathcal{N}_{s,\sigma}(\omega)$].

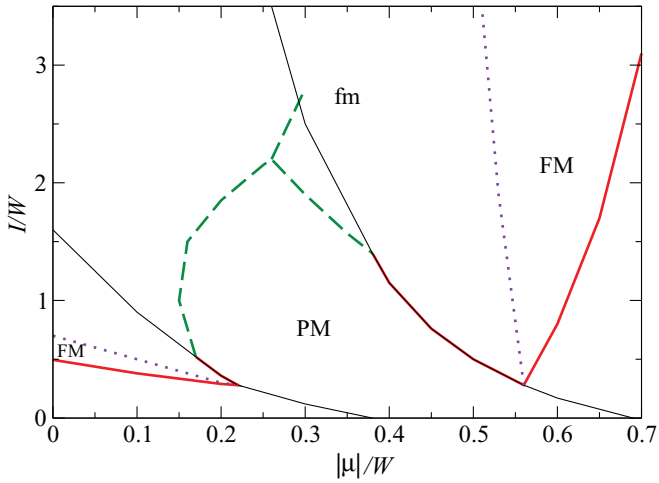

FIG. 2. (Color online) Phase diagram on the I/W vs $|\mu|/W$ plane at $T = 0$. The values of the other parameters are $\epsilon_d/W = -0.5$, $u/W^{1/2} = 1.0$, and $v/W^{3/2} = 0.05$. The labels fm, FM, and PM indicate the ferrimagnetic, ferromagnetic, and paramagnetic states, respectively. The thick solid (online red) line marks a second-order transition. The thick dashed (online green) line marks a first-order transition. The dotted (online violet) line marks the boundary between the fm and FM states (no phase transition occurs here; see text). In the region comprised between the two thin solid lines, a (meta)stable semiconducting PM state exists (see text).

characterizes the distribution of spectral weight, are shown in Fig. 1 and will be discussed below.

To characterize the spin polarization of the various phases, we define the dimensionless partial magnetizations

$$m_d \equiv \sum_\sigma \sigma n_{d,\sigma} = n_{d,\uparrow} - n_{d,\downarrow},$$

$$m_s \equiv \sum_\sigma \sigma n_{s,\sigma} = n_{s,\uparrow} - n_{s,\downarrow},$$

(by definition, $-1 \leqslant m_{d,s} \leqslant 1$) and the total magnetization $m_{\rm tot} \equiv m_d + m_s$ (with $m_{\rm tot} \neq 0$ in a spin-polarized state). The resulting phase diagram in the I/W vs $|\mu|/W$ plane is shown in Fig. 2. At $I = 0$ the only stable state is PM, with $m_{\rm tot} = 0$. A typical density of states of the PM state is shown in Fig. 1(a), and is characterized by equal distribution for the two spin projections $\sigma = \uparrow, \downarrow$ in the two confinement state bands. The upper confinement state band partially overlaps with the conduction band of the bulk semiconductor host, which is located at positive energy, $E_{\mathbf{K}} \geqslant 0$. A spin-polarized solution with $m_{\rm tot} \neq 0$ is found at each μ for sufficiently large I. Typical density of states corresponding to spin-polarized solutions of the self-consistency equations are shown in Figs. 1(b)–1(d), and are characterized by a different distribution of electrons with spin projection $\sigma = \uparrow$ [henceforth majority spins, assuming $m_{\rm tot} > 0$ (Ref. 14)] and $\sigma = \downarrow$ (minority spins), and by a significant redistribution of spectral weight in the minority spin band: with increasing I the upper minority spin band is pushed to higher energy until it gets completely embedded in the conduction band of the bulk semiconductor host, while the d weight is transferred to it at the expense of the d character of the lower minority spin band, whose s character thus increases [compare Figs. 1(a)–1(c)].

When $|\mu|/W \lesssim 0.55$, the spins of s electrons and the spins of d electrons are antiparallel (i.e., $m_d m_s < 0$) in the spin-polarized state. The corresponding density of states is shown in Figs. 1(b) and 1(c), from whence it is evident that this condition is achieved when the number of minority s spins exceeds the number of majority s spins. This is a consequence of the fact that, due to the Hubbard repulsion I, the minority spin band has mainly s character. Since s and d electron states, although confined in the vicinity of the magnetic δ layer, are spatially separated, the ground state of the system in this region of parameter space is *ferrimagnetic* (fm). For larger $|\mu|/W$ the number of majority s spins exceeds the number of minority s spins and the ground state of the system is *ferromagnetic* (FM), with $m_d m_s > 0$. A typical density of states for this case is shown in Fig. 1(d). A FM ground state is also found when $|\mu|/W \lesssim 0.25$, in a small region close to the transition to the *paramagnetic* (PM) state, where the upper majority spin band is partially filled and I is not too large, so that the d character of the minority spin band is sizable. We point out that the passage from a fm to a FM state (marked by a dotted line in Fig. 2) is not a phase transition, since no symmetry change is involved. This is clearly seen comparing the corresponding density of states, shown in Figs. 1(c) and 1(d), respectively. The two spectra are altogether similar and only differ in the filling of the lower minority spin band, so the passage from one state to the other is mainly controlled by μ, whereas I plays a little role, as is witnessed by the fact that the dotted line marking this passage in Fig. 2 is almost vertical.

A first-order phase transition and reentrant phenomena with increasing $|\mu|$ or I are observed in a window $0.15 \lesssim |\mu|/W \lesssim 0.35$, due to the presence of a competing insulating PM state, with μ falling within the gap between the upper and the lower two-dimensional band [the density of states of this insulating PM state is shown in Fig. 1(a)]. This state exists as a (meta)stable phase, i.e., as a (local) minimum of the thermodynamic grand-canonical potential Ω in the region delimited by the two thin lines in Fig. 2. Of course, in the region where the spin-polarized state is stable, the latter is characterized by a lower value (absolute minimum) of Ω. We point out that when μ is located within the gap between the the upper and the lower two-dimensional band, the electron filling does not change with changing the chemical potential (at $T = 0$). We shall come back to this point in Sec. III B.

The energy spectra of the spin-polarized states shown in Figs. 1(b)–1(d) display a half-metallic character, with full polarization of charge carriers at the Fermi level. This spin-polarized half-metallic state is found in a wide range of parameters. We pointed out that the variation of the number of particles with I at fixed μ and $I/W \gtrsim 2$ is altogether weak so that curves with a constant number of particles in the magnetic region of the phase diagram in Fig. 2 are almost vertical lines (the changes being at most 4%). Then, the properties of the spectra can be essentially described with varying μ at a generic $I/W \gtrsim 2$. At $-0.2 \lesssim \mu/W \leqslant 0$, a half-metallic state exists, with the Fermi level falling in the portion of the upper majority spin band located just below the threshold of the conduction band of the semiconductor host, while the lower majority and minority spin bands are full. Due to the partial overlap of the upper majority and lower minority spin bands, in the window $-0.3 \lesssim \mu/W \lesssim -0.2$ a spin-polarized metallic state exists. At $-0.6 \lesssim \mu/W \lesssim -0.3$, the half-metallic state reappears, with the Fermi level falling in the lower minority spin band, while the majority spin band is full. At $\mu/W \lesssim -0.6$ the lower majority and minority spin bands partially overlap and a FM metallic state exists.

B. Fixed number of particles

We now discuss the ground-state properties of the system at a fixed number of particles (i.e., when the system is described within the canonical statistical ensemble and the number of particles acts as a tunable control parameter), to obtain a complementary insight into the properties of the system. Our discussion is again limited to electron densities for which the chemical potential is located below the bottom of the three-dimensional band of the semiconductor host.

In the case of a fixed number of particles, the appropriate thermodynamical potential, which allows one to determine the most stable phase in the case of coexistence of different phases for the same set of parameters, is the free energy per transition-metal site,

$$F = \Omega + \mu n = \sum_{\substack{\alpha = s,d \\ \sigma = \uparrow,\downarrow}} \int_{-\infty}^{\mu} d\omega\, \omega\, \mathcal{N}_{\alpha,\sigma}(\omega) - I\, n_{d,\downarrow}\, n_{d,\uparrow},$$

where

$$n = \sum_{\substack{\alpha = s,d \\ \sigma = \uparrow,\downarrow}} n_{\alpha,\sigma} = \sum_{\substack{\alpha = s,d \\ \sigma = \uparrow,\downarrow}} \int_{-\infty}^{\mu} d\omega\, \mathcal{N}_{\alpha,\sigma}(\omega) \qquad (3)$$

is the total number of electrons in the δ layer per transition-metal site (hereafter called electron filling), and Eq. (3) must be numerically inverted to obtain the self-consistent value of the chemical potential μ corresponding to a given value of n.

In Fig. 3 we plot the phase diagram in the I/W vs n plane. Remarkably, the reentrant PM state in Fig. 2 is confined to a vertical segment at $n = 2$. This corresponds to the fact that this state is insulating, with the chemical potential falling within the gap between the upper and lower two-dimensional bands. Therefore, while this state extends over a finite window of values of $|\mu|/W$, its electron filling is fixed at $n = 2$ (the lower two-dimensional band is full and the upper two-dimensional band is empty). This insulating PM state separates at $I/W \lesssim 2.2$ a lower-density fm state (corresponding to larger values of $|\mu|/W$ in Fig. 2) and a higher-density fm state (corresponding to smaller values of $|\mu|/W$ in Fig. 2). Both states are generally half metallic, with the exchange splitting taking place in the lower or in the upper two-dimensional band. With decreasing n, the lower-density fm state turns into a FM state. The same holds for the higher-density FM state, with increasing n for $0.3 \lesssim I/W \lesssim 1$. For $I/W \lesssim 0.3$ the PM state is the only stable ground state at all electron fillings n.

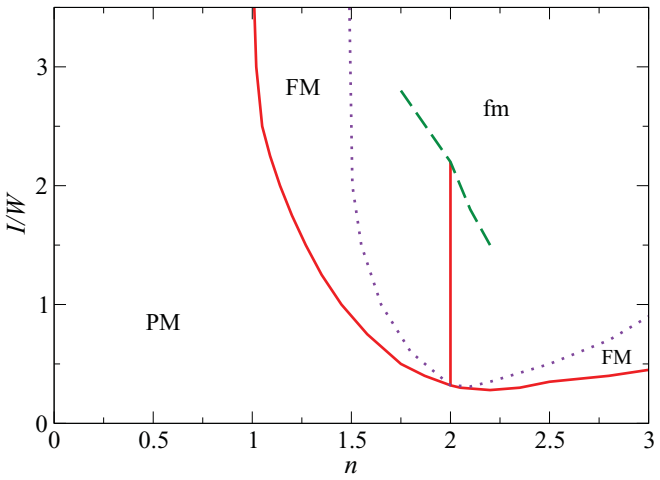

FIG. 3. (Color online) Phase diagram on the I/W vs n plane at $T = 0$. The values of the other parameters are $\epsilon_d/W = -0.5$, $u/W^{1/2} = 1.0$, and $v/W^{3/2} = 0.05$. The labels fm, FM, and PM indicate the ferrimagnetic, ferromagnetic, and paramagnetic states, respectively. The solid (online red) line marks a second-order transition. The dashed (online green) line marks a first-order transition. The dotted (online violet) line marks the boundary between the fm and FM states (no phase transition occurs here; see text). The semiconducting PM state at $n = 2$ separates a high-density and a low-density fm state.

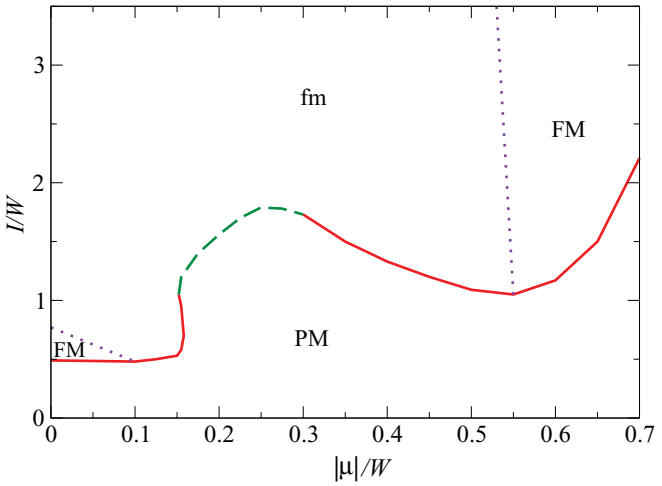

FIG. 4. (Color online) Phase diagram on the I/W vs $|\mu|/W$ plane at $T/W = 0.05$. The values of the other parameters are $\epsilon_d/W = -0.5$, $u/W^{1/2} = 1.0$, and $v/W^{3/2} = 0.05$. The labels fm, FM, and PM indicate the ferrimagnetic, ferromagnetic, and paramagnetic states, respectively. The solid (online red) line marks a second-order transition. The dashed (online green) line marks a first-order transition. The dotted (online violet) line marks the boundary between the fm and FM states (no phase transition occurs here; see text).

IV. FINITE TEMPERATURE

To study the properties of the system at finite temperature, we must solve the two coupled equations

$$n_{d,\sigma} = \int_{-\infty}^{+\infty} d\omega\, \mathcal{N}_{d,\sigma}(\omega) f(\omega - \mu), \tag{4}$$

for $\sigma = \uparrow, \downarrow$. Here, $f(z) = [e^{z/T} + 1]^{-1}$ is the Fermi-Dirac distribution function and T is the temperature (henceforth we measure the temperature in energy units, taking the Boltzmann constant $k_B = 1$). These equations can be treated and solved with the same procedure adopted in Sec. III A. Once the self-consistent values of $n_{d,\sigma}$ are obtained, we can proceed to calculate

$$n_{s,\sigma} = \int_{-\infty}^{+\infty} d\omega\, \mathcal{N}_{s,\sigma}(\omega) f(\omega - \mu).$$

Then, as usual, we can calculate the partial magnetizations $m_d \equiv n_{d,\uparrow} - n_{d,\downarrow}$, $m_s \equiv n_{s,\uparrow} - n_{s,\downarrow}$, and the total magnetization $m_{\rm tot} \equiv m_d + m_s$ to characterize the magnetic properties of the system.

Before starting our discussion of the properties of the model at finite temperature, a remark is mandatory. It is well known that the mean-field approach overestimates the critical temperature for the transition of the FM (or fm) state to the PM state. Actually, the mean-field critical temperature sets the scale for the formation of local moments. Their ordering, at a lower temperature, is instead controlled by the stiffness of spin fluctuations. We shall come back to this point in Sec. V.

A. Fixed chemical potential

At fixed chemical potential μ, to identify the most stable state in the case of coexistence of multiple phases for the same set of parameters, we need to calculate the thermodynamic grand-canonical potential per transition-metal site. We shall use the approximate expression

$$\Omega \approx -T \sum_{\substack{\alpha = s,d \\ \sigma = \uparrow,\downarrow}} \int_{-\infty}^{+\infty} d\omega\, \ln[1 + e^{(\mu-\omega)/T}]\, \mathcal{N}_{\alpha,\sigma}(\omega) - I\, n_{d,\downarrow}\, n_{d,\uparrow},$$

which is correct as long as the electron states involved have a vanishingly small inverse lifetime. This is exactly true for the two-dimensional confinement states which are not embedded in the three-dimensional continuum, but fails for the two-dimensional confinement states with positive energy. However, since our analysis is devoted to the case when the conduction band is empty at $T = 0$, the values of μ are always such that the main contribution to the thermodynamic grand-canonical potential comes from two-dimensional confinement states which are located below the threshold of the three-dimensional continuum. As a consequence, our approximate formula yields a thermodynamic grand-canonical potential with the correct properties (i.e., Ω is always lowest in the stable phase and is continuous at the transition point when the self-consistency equations yield a second-order phase transition).

In Fig. 4, we show the phase diagram for the same set of parameters as in Fig. 2, but for a finite temperature $T/W = 0.05$. It is evident that thermal effect tends to reduce the region where a first-order transition and reentrant phenomena are observed. This is connected to the fact that at finite temperature the filling of the PM phase changes continuously with the chemical potential even when μ falls within the gap between the upper and lower two-dimensional bands, as carriers can be thermally excited through the gap.

At $T/W = 0.1$ reentrant phenomena are suppressed and the phase transition line is monotonic, although hints of the low-

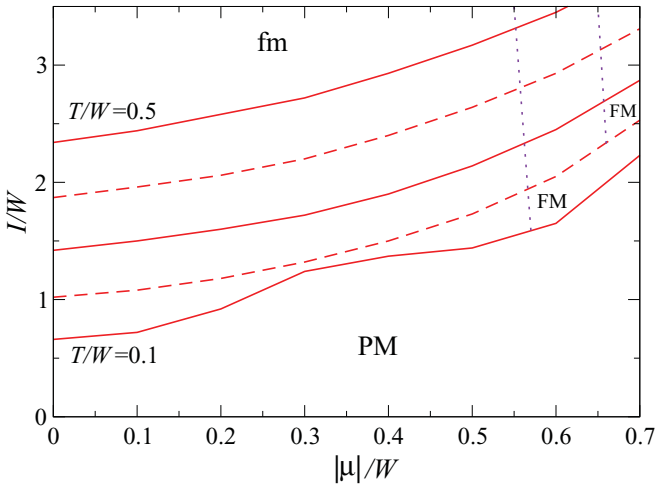

FIG. 5. (Color online) Phase diagrams on the I/W vs $|\mu|/W$ plane at $T/W = 0.1,0.2,0.3,0.4,0.5$. The values of the other parameters are $\epsilon_d/W = -0.5$, $u/W^{1/2} = 1.0$, and $v/W^{3/2} = 0.05$. The labels fm, FM, and PM indicate the ferrimagnetic, ferromagnetic, and paramagnetic states, respectively. All the transition (solid and dashed, online red) lines are second order and are alternated to make the figure easier to read. The dotted line (online, violet, visible in the given window only for $T/W = 0.1,0.2$) marks the boundary between the fm and FM states (no phase transition occurs here; see text).

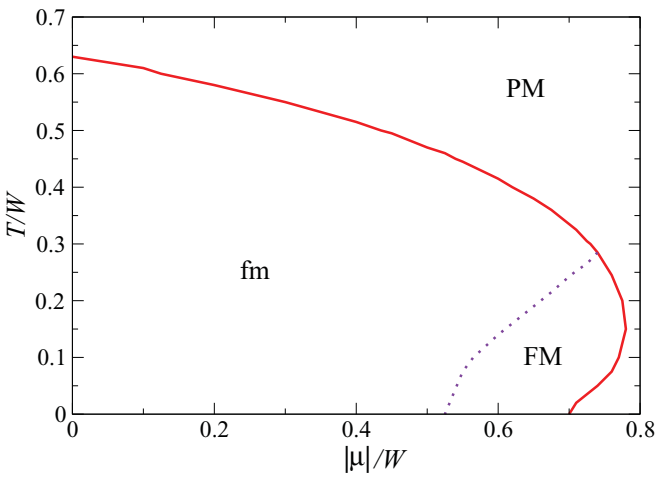

FIG. 6. (Color online) Phase diagram in the T/W vs $|\mu|/W$ plane at $I/W = 3.0$. The values of the other parameters are $\epsilon_d/W = -0.5$ and $v/W^{3/2} = 0.05$. The labels fm, FM, and PM indicate the ferrimagnetic, ferromagnetic, and paramagnetic states, respectively. The solid (online red) line marks a second-order transition. The dotted (online violet) line marks the boundary between the fm and FM states (no phase transition occurs here; see text).

temperature reentrant behavior are still visible in the change of curvature of the phase transition line. The transition from the PM phase to the fm or FM phase is always of second order (see Fig. 5). At $T/W > 0.2$ all traces of reentrant phenomena are washed out and the second-order transition line is a monotonic and convex function of $|\mu|/W$. As far as the FM phase is concerned, a temperature $T/W = 0.1$ is already enough to wash out the region of existence of the FM phase at $|\mu|/W \gtrsim 0$, whereas the FM phase at large $|\mu|/W$ is pushed further away as T/W is increased. As a result, the region of stability of the fm phase becomes wider with increasing temperature.

Finally, we want to discuss a typical phase diagram in the T/W vs $|\mu|/W$ plane, at a fixed value $I/W = 3.0$ (Fig. 6). The fm or FM ground states are gradually suppressed with increasing temperature for $0 \leqslant |\mu|/W \lesssim 0.70$. In this region, the critical temperature associated with the second-order phase transition to the PM phase is a monotonic decreasing function of $|\mu|/W$. Observe that the FM ground states evolve at a certain finite temperature into a fm phase, prior to the transition to the PM phase (consistently with the previous observation that the region of stability of the fm phase becomes wider with increasing temperature). Reentrance of the FM phase is observed in a small window $0.70 \lesssim |\mu|/W \lesssim 0.78$, where the ground state is PM, and the FM phase appears at finite temperature. In this region, a direct second-order transition from the FM phase back to the PM phase takes place at higher temperature. No spin-polarized phase exists for $|\mu|/W \gtrsim 0.78$.

B. Fixed number of particles

When the temperature is finite, the conditions that allow one to fix the number of particles in our system must be suitably specified. Indeed, an isolated magnetic δ layer cannot change the filling of the bulk semiconductor. In this sense, the chemical potential of the system should be assumed as fixed by the bulk, which acts as a particle reservoir for the magnetic δ layer. However, the case in which the filling n is fixed together with μ is physically meaningful. To realize this condition at finite T, when particles are thermally excited, we must imagine that the system reorganizes in such a way as to keep n fixed. As remarked in Sec. II, the physical parameter which controls the charge redistribution around the δ layer, to preserve charge neutrality, is the local correction to the chemical potential U. Within our simplified treatment, this parameter entails in an effective way the self-consistent redistribution of charge, which should be formally determined solving the Poisson equation. Therefore, at $T = 0$, we have fixed the value of U that corresponded to some assumedly self-consistent charge redistribution. To keep n fixed at $T > 0$ we must allow U to vary. Its value must be fixed by the condition which guarantees that charge neutrality assumedly achieved at $T = 0$ is not violated by thermal excitations.

As is seen in Fig. 7, where the temperature evolution of the magnetization in the case $n = 1.5$, $\mu/W = -0.4$ is shown, the variation of $u(T)/W^{1/2}$ in the whole temperature range where the fm phase exists does not exceed 10% of the average value $u/W^{1/2} \approx 1.0$.

V. THERMODYNAMICAL FLUCTUATIONS

So far, we have discussed the mean-field properties of our model for a semiconductor with a magnetic δ layer. Although embedded into the three-dimensional semiconductor host, the magnetic δ layer and the spin-polarized confinement states associated with it are intrinsically two dimensional. Then, thermodynamical fluctuations are expected to play a crucial role. In the case of a genuinely isotropic exchange coupling between the magnetic moments, like the one considered in our model [the I term in Eq. (1) does not fix the local quantization

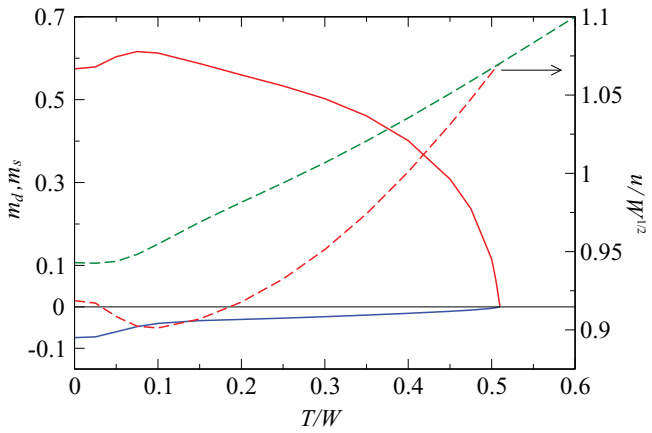

FIG. 7. (Color online) (To be read on the left axis, solid lines.) Variation of the dimensionless partial magnetizations m_d (>0, online red) and m_s (<0, online blue) as a function of T/W in the fm state at $I/W = 3.0$, $n = 1.5$, and $\mu/W = -0.4$. The values of the other parameters are $\epsilon_d/W = -0.5$ and $v/W^{3/2} = 0.05$. (To be read on the right axis, dashed lines.) Variation of the parameter $u/W^{1/2}$, ruling charge neutrality, as a function of T/W, for the same set of parameters, in the PM (upper line, online green) and in the fm (lower line, online red) state.

axis], these fluctuations are expected to completely wash out the mean-field magnetic order. However, small relativistic effects and dipole-dipole interactions introduce a magnetic anisotropy in real systems. This anisotropy may be of the Ising (easy-axis) type or of the XY (easy plane) type. In both cases, the mean-field transition temperature T_{mf} must be interpreted as a temperature scale for the formation of the local magnetic moments, whereas the temperature T_c ($\ll T_{mf}$) for their ordering (of Ising or Kosterliz-Thouless type) is ruled by the stiffness of spin fluctuations. To estimate T_c, we therefore calculated the longitudinal and transversal spin stiffness (J_L and J_T, respectively), which are obtained by an expansion at small wave vectors $\mathbf{q}$ of the longitudinal and transverse bare spin susceptibilities,

$$X_L(\mathbf{q}) \equiv X_{zz}(\mathbf{q}) = \frac{I^2}{4N_\parallel}\sum_{\mathbf{k},\sigma}\int_{-\infty}^{+\infty}\frac{d\omega}{2\pi i} \times G_{dd,\sigma}(\zeta_\omega,\mathbf{k}_+)G_{dd,\sigma}(\zeta_\omega,\mathbf{k}_-),$$

$$X_T(\mathbf{q}) \equiv X_{xx}(\mathbf{q}) = X_{yy}(\mathbf{q}) = \frac{I^2}{4N_\parallel}\sum_{\mathbf{k},\sigma}\int_{-\infty}^{+\infty}\frac{d\omega}{2\pi i} \times G_{dd,\sigma}(\zeta_\omega,\mathbf{k}_+)G_{dd,-\sigma}(\zeta_\omega,\mathbf{k}_-),$$

calculated at $T = 0$ in the spin-polarized (fm or FM) phase. Here, $\zeta_\omega \equiv \omega + i\delta\,\mathrm{sgn}\,\omega$, $\mathbf{k}_\pm \equiv \mathbf{k} \pm \frac{1}{2}\mathbf{q}$. After numerical evaluation of the bare spin susceptibilities, the longitudinal and transverse spin stiffnesses are then found through the relations $X_L(\mathbf{q}) = X_L(0) + J_L\mathbf{q}^2$, $X_T(\mathbf{q}) = X_T(0) + J_T\mathbf{q}^2$ (wave vectors are expressed here in units of the inverse lattice spacing $1/a^*$).

We essentially devote our discussion to the half-metallic state which exists at $T = 0$ in the range $-0.6 \lesssim \mu/W \lesssim -0.3$, where the lower minority spin band is partially filled and the lower majority spin band is full, since this is the case which seems to be relevant to interpret the outcomes of numerical calculations. In this region, J_L is positive and large ($J_L/W \approx 3.0$), indicating that fluctuations in the amplitude of the magnetization m_d can be neglected.

For small $I/W \lesssim 3.0$, J_T turns out to be negative, while $X_T(\mathbf{q})$ develops a minimum at some finite $\mathbf{q}$, indicating the occurrence of a noncollinear fm (or FM) state with an incommensurate canting of magnetic moments.

At $I/W \gtrsim 3.0$, J_T is positive and decreases with decreasing number of particles n. For instance, $J_T/W = 0.25,0.23,0.20$ for typical numbers of particles in the half-metallic phase $n = 1.57,1.52,1.45$, respectively. Therefore, the collinear fm (or FM) state is stable against canting of the magnetic moments. In this region of parameters, the mean-field transition temperature is on the order of $T_{mf}/W \approx 0.5$ for, e.g., $I/W = 3.0$, and increases with increasing I ($\Delta T_{mf}/\Delta I \approx 0.5$). At the coverage reached in experimental conditions we can estimate $a^*/a \approx 2$–3 and $W \approx 0.1$–0.2 eV. Then, $T_{mf} \approx 500$–1000 K. This is the temperature scale for the formation of local moments. The real transition temperature, ruled by thermodynamical fluctuations, may be estimated as $T_{\mathrm{Ising}} \approx 2J_T m_d^2/\log(1+\sqrt{2})$ in the Ising (easy-axis) case, or $T_{XY} \approx \pi J_T m_d^2/2$ in the XY (easy-plane) case, with $m_d \approx 0.5$ in this region of parameters. As a consequence, $T_{\mathrm{Ising}}/W \approx 0.1$ and $T_{XY}/W \approx 0.075$, i.e., $T_{\mathrm{Ising}} \approx 100$–$200$ K and $T_{XY} \approx 75$–150 K. The change of critical temperature with changing the number of particles in the half-metallic state is

$$\frac{\Delta T_c}{T_c} = 2.5\frac{\Delta n}{n},$$

with $T_c = T_{\mathrm{Ising}}$ or $T_c = T_{XY}$, in the easy-axis or easy-plane case, respectively. If one considers only the number of free carriers in the half-metallic state, $n_{\mathrm{free}} = n - 1$ (one electron per transition-metal site is located in the completely filled lower majority-spin band), the estimate

$$\frac{\Delta T_c}{T_c} = 0.8\frac{\Delta n}{n_{\mathrm{free}}}$$

is obtained.

We may now attempt a comparison between our results and existing numerical and experimental results. *Ab initio* calculations for a regular array of δ layers obtain an estimate for the ground-state spin stiffness, which is subsequently used to obtain an estimate for the critical temperature within Monte Carlo simulations of the resulting effective (anisotropic) Heisenberg model.[15,16] In Ref. 15, the critical temperature for the Ge/Mn system is estimated as $T_c \approx 200$–300 K, which compares well with our result in the Ising (easy-axis) case. The experimental critical temperature is somewhat smaller, $T_c \approx 40$–50 K.[2] These results are not unexpected: our model captures the main ingredients of *ab initio* calculations, and we only need to take into account thermodynamical spin fluctuations to obtain the reduction of the critical temperature from the exceedingly high mean-field value to a reasonable value. However, both our model and *ab initio* calculations miss the effect of disorder in the magnetic system, which is expected to further reduce the critical temperature, down to the value observed experimentally.

VI. SYSTEMS WITH A QUANTUM-WELL CARRIER CHANNEL

Although we have shown that our model of magnetic ordering in an isolated δ layer embedded into a semiconductor host captures the relevant outcomes of numerical calculations and can account for the magnetic properties observed in experiments,[2] it is of interest to briefly discuss here some aspects of this ordering in more complex systems, where the strength of the interaction between (s,p) free carrier spins and $3d$-magnetic ion spins can be varied locally. For example, III-V DMHs of this type have been grown and studied, in which a δ layer of Mn was deposited close to a quantum well (also called channel) at some distance (called spacer) d from it.[4–6]

The effect of the channel on magnetism in such multicomponent systems is threefold. First, the quantum magnetic proximity effect (interpenetration of the wave function tails both into the channel and into the δ layer) modifies the effective exchange integral between the local spins of magnetic ions in the δ layer and polarizes the free carrier spins in the channel.[4] Second, quantum fluctuations in the channel stabilize FM order in the δ layer, while suppressing the amplitude of the magnetic moment and the transition temperature with respect to those found within the mean-field approach.[17] Third, electrostatic charge redistribution between the δ layer and the channel occurs, due to their different density of states and deepness; this entails a modification of the magnetic characteristics of the δ layer, on purely classical grounds, even without quantum magnetic proximity effect.

In this paper, we shall not discuss all the aspects of the very complex problem of magnetism in DMHs with a magnetic δ layer and a nonmagnetic channel, but limit ourselves to a qualitative analysis of the effect of spin polarization of the δ layer on the charge redistribution between them. Henceforth, we indicate with n_δ the number of particles per two-dimensional unit cell in the δ layer and with n_c the number of particles per two-dimensional unit cell in the channel, and consider the situation where, along with the chemical potential μ, which is fixed by the bulk, also the total number of particles $n = n_\delta + n_c$ is fixed, as we did in Sec. IV B, in the case $n_c = 0$ (absence of channel, i.e., $n_\delta = n$).

The channel itself is described as a quantum well, where confinement in the perpendicular direction introduces a quantization of the energy levels, which form subbands $\varepsilon^\varsigma_{\mathbf{k}}$, where $\varsigma = 0,1,2,\ldots$ is the subband index. We limit ourselves to consider the case when the lowest subband $\varepsilon^0_{\mathbf{k}} \equiv E_0 + \hbar^2\mathbf{k}^2/(2m_c)$ is filled. We assume that the effective mass approximation is valid in the lowest subband, and indicate with m_c the effective mass of carriers in the channel. In the following, this band will be simply described through a constant density of states per two-dimensional unit cell ϱ_0.

The position of the bottom of this band, with respect to the confinement states which are formed around the δ layer, is ruled by the Coulomb energy involved in the charge redistribution, and to take into account this effect we adopt a simple capacitive model

$$E_0 = \bar{E}_0 + U - \gamma d(n - n_\delta),$$

where $\bar{E}_0$ is a constant fixing the position of the bottom of the band in the absence of the δ layer, $\gamma d/e^2$ is an inverse capacitance per two-dimensional unit cell, d is the distance between the δ layer and the channel, e is the electron charge, and $n_\delta + n_c = n$. The model assumes that, in the absence of the channel ($\varrho_0 = 0$), charge neutrality is achieved in correspondence of the value of U at which $n_\delta = n$ (see Sec. IV B). The inverse capacitance coefficient may be roughly estimated as

$$\gamma \approx \frac{e^2}{\epsilon_0\epsilon_r(a^*)^2},$$

where ϵ_0 is the vacuum dielectric constant, and ϵ_r is the relative dielectric constant of the semiconducting host. Thus, $e^2/(\gamma d) = \epsilon_0\epsilon_r(a^*)^2/d$, and γd is an energy scale. When the channel is partially filled at $T = 0$, we have $E_0 < 0$.

The number of carriers per two-dimensional unit cell in the channel is

$$n_c = \varrho_0 T\ \ln[1 + e^{(\mu - E_0)/T}]. \tag{5}$$

Of course, when $\mu - E_0 \gg T$, the approximate relation $n_c \approx \varrho_0(\mu - E_0)$ holds. In typical experimental conditions, the number of particles in the channel is much smaller than the number of particles in the δ layer ($n_c/n_\delta \approx 0.01$–$0.05$). Equation (5) must be solved self-consistently, together with Eqs. (4), to yield a value of u such that n remains constant.

To reproduce the results of the experiments, at least qualitatively, we have taken $\bar{E}_0/W = -1.0$, $\gamma d/W = 1.0$, $\varrho_0 W = 0.025, n = 1.5, I/W = 3.0$, and $\mu/W = -0.4$. These parameters yield $n_c/n_\delta \approx 0.027$ at $T = 0$.

In Fig. 8 we show that n_δ decreases with T, except at very low temperature, where the nonmonotonic behavior of m_d (similar to the one reported in Fig. 7, since the presence of the channel with a small density of states introduces small corrections) is reflected in a tiny increase of n_δ. Of course, the opposite behavior is observed in $n_c = n - n_\delta$. It should be kept in mind that, although the absolute variations are, of course, the same, $|\Delta n_\delta| = |\Delta n_c|$, the relative variations are much different, $|\Delta n_\delta|/n_\delta \ll |\Delta n_c|/n_c$. For instance, taking as a reference the values at the PM-fm transition, and measuring the variations at $T = 0$ we have $|\Delta n_\delta|/n_\delta \approx 0.003$ and $|\Delta n_c|/n_c \approx 0.08$. We recall that in the half-metallic state we are considering the number of free carriers in the δ layer is $n_{\text{free}} = n_\delta - 1$, since one particle occupies the completely filled lower majority-spin band.

It is interesting to note the change of slope at the PM-fm transition point. Thus, with lowering the temperature, particles migrate from the channel toward the δ layer, and the rate of migration increases below the transition temperature.

In Fig. 9 we show the behavior of n_δ and n_c with varying the spacer thickness d (i.e., the distance between the δ layer and the channel). We find that n_δ monotonically decreases with increasing d (whereas, of course, $n_c = n - n_\delta$ increases). However, it should be kept in mind that below a certain distance d^* our approximation of a sharp δ layer breaks down.

As far as the variations are concerned, we point out again that, although the absolute variations are the same, $|\Delta n_\delta| = |\Delta n_c|$, the relative variations are much different, $|\Delta n_\delta|/n_\delta \ll |\Delta n_c|/n_c$. For instance, taking as a reference the values at $\gamma d/W = 1$, and measuring the variations at $\gamma d/W = 10$ we have $|\Delta n_\delta|/n_\delta \approx 0.007$ and $|\Delta n_c|/n_c \approx 0.26$.

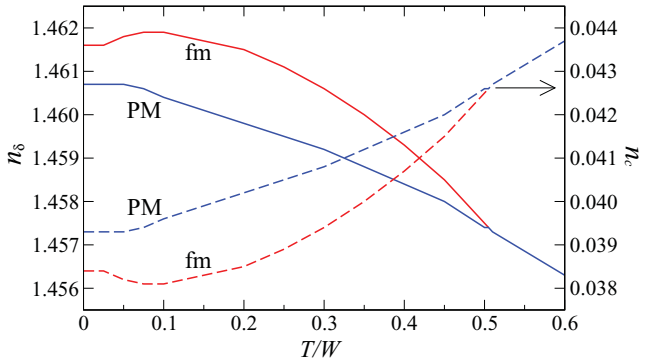

FIG. 8. (Color online) (To be read on the left axis, solid lines.) Variation of the number of particles in the δ layer per two-dimensional unit cell, n_δ, in the fm (online red line) and PM (online blue line) phases, as a function of T/W, at $I/W = 3.0$, $n = 1.5$, and $\mu/W = -0.4$. The values of the other parameters are $\epsilon_d/W = -0.5$, $v/W^{3/2} = 0.05$, $\bar{E}_0/W = -1.0$, $\gamma d/W = 1.0$, and $\varrho_0 W = 0.025$. (To be read on the right axis, dashed lines.) Variation of the number of particles in the channel per two-dimensional unit cell, n_c, in the fm (online red line) and PM (online blue line) phases, as a function of T/W, for the same set of parameters.

VII. SUMMARY AND CONCLUDING REMARKS

Our Anderson-like model captures the main ingredients of the physics of a magnetic δ layer in a semiconductor host and is therefore able to account for the occurrence of a spin-polarized half-metallic behavior in the system. This is the cooperative result of hybridization of electron states in the layer and the host, and also of charge and spin redistribution around the δ layer, giving rise to two-dimensional confinement-state bands which undergo full exchange splitting for physically reasonable values of the exchange coupling. We have shown that the magnetic characteristics can be ascribed to a single δ layer,[7] while their periodical arrangement, or the introduction of a quantum-well carrier channel should introduce some modifications in our description.

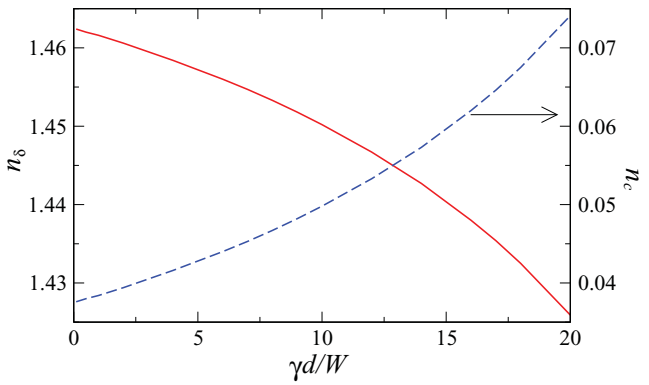

FIG. 9. (Color online) (To be read on the left axis, solid online red line.) Variation of the number of particles in the δ layer per two-dimensional unit cell, n_δ, in the fm phase at $T = 0$, as a function of $\gamma d/W$, at $I/W = 3.0$, $n = 1.5$, and $\mu/W = -0.4$. The values of the other parameters are $\epsilon_d/W = -0.5$, $v/W^{3/2} = 0.05$, $\bar{E}_0/W = -1.0$, and $\varrho_0 W = 0.025$. (To be read on the right axis, dashed online blue line.) Variation of the number of particles in the channel per two-dimensional unit cell, n_c, in the fm phase at $T = 0$, as a function of $\gamma d/W$, for the same set of parameters.

Of course, our model misses some aspects of the numerical calculations,[8–12] such as the orbital degeneracy, the crystal-field splitting, and details of the lattice band structure beyond the effective mass approximation. These aspects can be accounted for in a straightforward way, by proper generalizations of the starting model, equipping the various lattice bands with orbital labels and considering the various hybridizations of (s,p) and d bands allowed by symmetry. However, the subsequent analysis of the model would require much heavier numerical effort, making the results less transparent. Further lines of investigation include the mechanism of exchange coupling among different δ layers when they are organized into a periodic structure,[2,3] and the feedback of the channel on the magnetic properties of the δ layer.[4–7]

As far as the first aspect is concerned, to evaluate the exchange interaction between two magnetic δ layers, in Ref. 18 we introduced a phenomenological model which assumed FM order within each δ layer as the starting point, and showed that there are two main mechanisms, which lead to the competition of FM and AFM coupling between two neighboring δ layers. The first interaction, mediated by mobile carriers in the two-dimensional confinement-state bands, is FM when the δ layers are close enough, but changes sign with increasing interlayer distance, becoming AFM. A further change of sign, back to FM, is also possible at even larger distances, depending on the values of the model parameters. The second interaction, mediated by interband virtual transitions between three-dimensional bands, may oscillate with the distance and is modulated by an exponentially decreasing prefactor. The case of a periodic array of magnetic δ layers could be studied within a suitable generalization of the model presented in this paper, which would allow one to treat intra- and interlayer exchanges on equal footing.

As far as the physics of systems with a channel is concerned,[4–6] in the absence of clear experimental indications, we can provide some indicative predictions about the behavior of the FM critical temperature T_c with varying distance d between the channel and the δ layer. In Sec. V we noticed that, in the half-metallic state, T_c is a decreasing function of the number of carriers in the δ layer, n_δ, which is in turn a decreasing function of the distance d between the channel and the δ layer (see Sec. VI). As a result, we expect T_c to decrease with d. In our model with a sharp profile of the δ layer, there is no lower limit for d. In real systems, instead, the profile of the δ layer is smeared, due to interdiffusion, so that our prediction is not valid when d becomes of the same order as the typical width of the smeared δ layer. In such conditions the channel and the δ layer must be considered as a unique metallic system, with the density of states composed of two contributions, coming from light and heavy carriers. At this point T_c is expected to decrease with further reducing d. So, we predict a nonmonotonic behavior of $T_c(d)$. We also predict (see Sec. VI) that n_δ increases in the spin-polarized (fm or FM) phase with respect to the PM phase, i.e., with lowering the temperature below the PM-fm (or FM) transition temperature, the rate of migration of carriers from the channel to the δ layer, even at the fixed spacer thickness, should increase.

ACKNOWLEDGMENTS

The work was partially supported by the University of the Basque Country (Proyecto GV UPV/EHU Grant No. IT-366-07), Spanish Ministerio de Ciencia y Tecnologia (Grant No. FIS2007-66711-C02-01), and by RFBR (Grant No. 10-02-0018-a). S.C. also acknowledges financial support by PRIN 2007 under Project No. 2007FW3MJX003. V.V.T. acknowledges financial support by Ikerbasque (Basque Foundation for Science).

[1] A. M. Nazmul, S. Sugahara, and M. Tanaka, Phys. Rev. B **67**, 241308(R) (2003); A. M. Nazmul, T. Amemiya, Y. Shuto, S. Sugahara, and M. Tanaka, Phys. Rev. Lett. **95**, 017201 (2005); B. A. Aronzon, A. S. Lagutin, V. V. Ryl'kov, V. V. Tugushev, V. N. Men'shov, A. V. Lashkul, R. Laiho, O. V. Vikhrova, Yu. A. Danilov, and B. N. Zvonkov, JETP Lett. **87**, 164 (2008).

[2] R. K. Kawakami, E. Johnston-Halperin, L. F. Chen, M. Hanson, N. Guébels, J. S. Speck, A. C. Gossard, and D. D. Awschalom, Appl. Phys. Lett. **77**, 2379 (2000).

[3] H. Luo, B. D. McCombe, M. H. Na, K. Mooney, F. Lehmann, X. Chen, M. Cheon, S. M. Wang, Y. Sasaki, X. Liu, and J. K. Furdyna, Physica E **12**, 366 (2002); X. Chen, M. Na, M. Cheon, S. Wang, H. Luo, B. D. McCombe, X. Liu, Y. Sasaki, T. Wojtowicz, J. K. Furdyna, S. J. Potashnik, and P. Schiffer, Appl. Phys. Lett. **81**, 511 (2002); B. D. McCombe, M. Na, X. Chen, M. Cheon, S. M. Wang, H. Luo, X. Liu, Y. Sasaki, T. Wojtowicz, J. K. Furdina, S. J. Potashnik, and P. Schiffer, Physica E **16**, 90 (2003).

[4] R. C. Myers, A. C. Gossard, and D. D. Awschalom, Phys. Rev. B **69**, 161305(R) (2004).

[5] M. V. Dorokhin, Yu. A. Danilov, P. B. Demina, V. D. Kulakovskii, O. V. Vikhrova, S. V. Zaitsev, and B. N. Zvonkov, J. Phys. D: Appl. Phys. **41**, 245110 (2008); S. V. Zaitsev, V. D. Kulakovskii, M. V. Dorokhin, Yu. A. Danilov, P. B. Demina, M. V. Sapozhnikov, O. V. Vikhrova, and B. N. Zvonkov, Physica E **41**, 652 (2009).

[6] B. A. Aronzon, M. A. Pankov, V. V. Rylkov, E. Z. Meilikhov, A. S. Lagutin, E. M. Pashaev, M. A. Chuev, V. V. Kvardakov, I. A. Likhachev, O. V. Vihrova, A. V. Lashkul, E. Lähderanta, A. S. Vedeneev, and P. Kervalishvili, J. Appl. Phys. **107**, 023905 (2010).

[7] O. V. Vikhrova, Yu. A. Danilov, M. V. Dorokhin, B. N. Zvonkov, I. L. Kalent'eva, and A. V. Kudrin, Pis'ma v JTF **35**, 8 (2009) (in Russian).

[8] S. Sanvito and N. A. Hill, Phys. Rev. Lett. **87**, 267202 (2001); Gefei Qian, Yia-Chung Chang, and J. R. Tucker, Phys. Rev. B **71**, 045309 (2005); M. C. Qian, C. Y. Fong, and W. E. Pickett, J. Appl. Phys. **99**, 08D517 (2006); X. H. Zhou, Xiaoshuang Chen, Y. Huang, H. Duan, L. Z. Sun, and W. Lu, *ibid.* **99**, 113903 (2006).

[9] M. M. Otrokov, V. V. Tugushev, A. Ernst, S. A. Ostanin, V. M. Kuznetsov, and E. V. Chulkov, JETP **112**, 625 (2011).

[10] A. Continenza, F. Antoniella, and S. Picozzi, Phys. Rev. B **70**, 035310 (2004); H.-Y. Wang and M. C. Qian, J. Appl. Phys. **99**, 08D705 (2006).

[11] M. C. Qian, C. Y. Fong, Kai Liu, W. E. Pickett, J. E. Pask, and L. H. Yang, Phys. Rev. Lett. **96**, 027211 (2006).

[12] H. Wu, P. Kratzer, and M. Scheffler, Phys. Rev. Lett. **98**, 117202 (2007).

[13] S. Caprara, V. V. Tugushev, P. M. Echenique, and E. V. Chulkov, Europhys. Lett. **85**, 27006 (2009).

[14] Of course, an equivalent solution of the self-consistency equations exists, with $m_{\text{tot}} < 0$.

[15] M. M. Otrokov, A. Ernst, S. Ostanin, G. Fischer, P. Buczek, L. M. Sandratskii, W. Hergert, I. Mertig, V. M. Kuznetsov, and E. V. Chulkov, Phys. Rev. B **83**, 155203 (2011).

[16] M. M. Otrokov, A. Ernst, V. V. Tugushev, S. Ostanin, P. Buczek, L. M. Sandratskii, G. Fischer, W. Hergert, I. Mertig, V. M. Kuznetsov, and E. V. Chulkov (unpublished).

[17] R. G. Melko, R. S. Fishman, and F. A. Reboredo, Phys. Rev. B **75**, 115316 (2007).

[18] V. N. Men'shov, V. V. Tugushev, P. M. Echenique, S. Caprara, and E. V. Chulkov, Phys. Rev. B **78**, 024438 (2008).